Biomedicine & Pharmacotherapy 109 (2019) 293–303

Contents lists available at ScienceDirect

Biomedicine & Pharmacotherapy

journal homepage: www.elsevier.com/locate/biopha

Mechanistic approach of the inhibitory effect of chrysin on inflammatory and apoptotic events implicated in radiation-induced premature ovarian failure: Emphasis on TGF-β/MAPKs signaling pathway

Eman M. Mantawy[a], Riham S. Said[b,*], Amal Kamal Abdel-Aziz[a]

[a] Pharmacology and Toxicology Department, Faculty of Pharmacy, Ain Shams University, Cairo, Egypt
[b] Drug Radiation Research Department, National Center for Radiation Research and Technology, Atomic Energy Authority, Cairo, Egypt

ARTICLE INFO

Keywords:
Ovarian failure
Radiotherapy
Chrysin
Apoptosis
Inflammation
MAPKs

ABSTRACT

Radiotherapy is one of the most relevant treatment modalities for various types of malignancies. However, it causes premature ovarian failure (POF) and subsequent infertility in women of reproductive age; hence urging the development of effective radioprotective agents. Chrysin, a natural flavone, possesses several pharmacological activities owing to its antioxidant, anti-inflammatory and anti-apoptotic properties. Therefore, the aim of this study was to investigate the efficacy of chrysin in limiting γ-radiation-mediated POF and to elucidate the underlying molecular mechanisms. Immature female Sprague-Dawley rats were subjected to a single dose of γ-radiation (3.2 Gy) and/or treated with chrysin (50 mg/kg) once daily for two weeks before and three days post-irradiation. Chrysin prevented the radiation-induced ovarian dysfunction by restoring estradiol levels, preserving the normal ovarian histoarchitecture and combating the follicular loss. Eelectron microscopic analysis showed that the disruption of ultrastructure components due to radiation exposure was hampered by chrysin administration. Mechanistically, chrsyin was able to reduce the levels of the inflammatory markers NF-κB, TNF-α, iNOS and COX-2 in radiation-induced ovarian damage. Chrysin also exhibited potent anti-apoptotic effects against radiation-induced cell death by downregulating the expression of cytochrome c and caspase 3. Radiation obviously induced upregulation of TGF-β protein with subsequent phospholyration and hence activation of downstream mitogen-activated protein kinases (MAPKs); p38 and JNK. Notably, administration of chrysin successfully counteracted these effects. These findings revealed that chrysin may be beneficial in ameliorating radiation-induced POF, predominantly via downregulating TGF-β/MAPK signaling pathways leading subsequently to hindering inflammatory and apoptotic signal transduction pathways implicated in POF.

1. Introduction

The World Health Organization recently stated that about 70% of the world's cancer-related deaths occur in middle and lowincome countries, including Africa [1]. Although radiotherapy is one of the most relevant treatment options for approximately 70% of cancer patient during the course of their treatment, there are acute and long term impediments following exposure to ionizing radiation [2]. Seriously, rapid ovarian dysfunction has been observed in young females after initiation of radiotherapy through accelerating menopause leading to permanent infertility in 55%–80% of patients before puberty [3]. Hence, as survival rates for young cancer patients continue to increase, the strategy of management has been changed from cure with any cost to improving the quality of life [4].

A multitude of molecular mechanisms are involved in the pathogenesis of radiation-induced toxicity, one of these critical mechanisms is the inflammatory cascade [5]. Post-radiation, a cascade of inflammatory reactions are initiated in the surrounding tissue resulting in production of numerous pro-inflammatory cytokines and chemokines which further perpetuate a long term inflammation and tissue injury. Of particular importance, transforming growth factor (TGF)-β plays crucial roles in the pathophysiology of various normal tissues toxicities associated with radiotherapy [6]. Although, inflammation plays a key physiological role in folliculogenesis and ovulation, aberrant inflammation can result in impaired oocyte quality, premature ovarian failure (POF), and associated infertility [7,8].

Beside inflammatory process, the apoptotic signaling pathways are critically recognized as the main cause of several deleterious effects associated with radiotherapy [9]. Remarkably, apoptosis is the main pathway of the attrition of the ovarian primordial follicle pool to

* Corresponding author at: Pharmacology & Toxicology, National Center for Radiation Research & Technology, Egyptian Atomic Energy Authority, Cairo, Egypt.
E-mail address: riham.said@eaea.org.eg (R.S. Said).

https://doi.org/10.1016/j.biopha.2018.10.092
Received 28 August 2018; Received in revised form 14 October 2018; Accepted 15 October 2018

eliminate defective oocytes [10,11]. Prior to menopause, quiescent primordial follicles are continuously recruited into the growing pool and pass through different stages of growth to ovulate oocytes. However, more than 95% of these follicles undergo atresia before reaching the pre-ovulatory follicle stage [12]. Ionizing radiation delivered to the cancer tissue produces toxic free radicals and reactive oxygen species which attack critical macromolecules such as DNA and disrupt mitochondrial membrane integrity, switching on the intrinsic pathway of apoptosis [13]. Crucially, the rate of follicle atresia can be accelerated by exposure to ionizing radiation, leading to early onset of ovarian senescence [14]. Thus, in addition to inflammation, apoptosis plays a critical role in regulating the ovarian function, which influence the length of a women's fertile lifespan and the timing of menopause.

In this context, there is a great necessity for exploring radioprotectors with the ability to prohibit the adverse effects associated with radiotherapy. Research endeavors with synthetic radioprotectors in the past have been met with little success primarily due to toxicity-related problems. Therefore, researchers diverted their attention toward phytochemicals as radioprotector due to their relatively better safety profile [15]. Flavonoids, a naturally occurring polyphenolic compound, have been reported to possess radioprotective activities by different mechanisms [16,17]. Interestingly, flavonoids were stated to be effective in preventing POF-induced by chemotherapy and radiotherapy through decreasing oxidative stress and apoptosis [8,18]. One of the promising compounds belonging to flavonoids family is chrysin (5,7-dihydroxyflavone) which is extracted from honey, propolis, and various plants [19]. Recent studies have revealed the numerous biological properties of chrysin including antioxidant, anti-apoptotic [20], anti-inflammatory [21,22], and anti-cancer [23]. Moreover, chrysin was reported to protect keratinocytes from UV radiation toxicity through attenuating ROS overproduction, COX2 induction and apoptosis [19]. Additionally, chrysin protected mice from lethal effects of whole-body γ-radiation, diminished primary DNA damage in leucocytes [24], as well as reduced radiation-induced mortality [25]. This, in turn points out that chrysin can be beneficial in abrogating ovarian damage and infertility induced by radiotherapy.

Consequently, the aim of this study was to explore the temporal pattern of ovarian toxicity post-radiation exposure and to investigate whether chrysin administration could be effective in the preservation of the ovarian function damaged by γ-radiation exposure, besides elucidating the underlying molecular mechanisms focusing on inflammatory, apoptotic and TGF-β signaling pathways.

2. Materials & methods

2.1. Chemicals and reagents

Chrysin was purchased from Sigma (St. Louis, MO). It was dissolved in a mixture of DMSO and corn oil at ratio (1:19). Estradiol ELISA kit was obtained from Monobind Inc. (Lake Forest, USA). Rat tumor necrosis factor (TNF)-α ELISA kit was secured from Assaypro (Assaypro Co, USA). Rat TGF-β kit was procured from Cusabio Biotech Co. (Wuhan, China). All other commercially available chemicals and solvents were of the highest grade.

2.2. Animals

Three-week-old female Sprague–Dawley (SD) rats, weighing 40–50 g, were purchased from Nile Co. for Pharmaceutical and Chemical industries, Egypt. Rats were housed in a controlled environment under an illumination schedule of 12 h light/12 h dark with controlled room temperature (25^{O}C). They were kept on a standard diet pellet containing not less than 20% protein, 5% fiber, 3.5% fat, 6.5% ash and a vitamin mixture. All procedures were operated according with the NIH Guide for the Care and Use of Laboratory Animals approved by the ethical guidelines of Faculty of Pharmacy, Ain Shams University, Cairo, Egypt.

2.3. Experimental design and establishment of POF model

Sixty female SD rats were divided into 4 groups of 15 rats each and treated for 17 consecutive days as follows; the first control and the second irradiated groups received the mixture of DMSO and corn oil, the vehicle of chrysin, (5 ml/kg B.W., P.O), once daily. The third and fourth groups were orally administered chrysin (50 mg/kg B.W.), once daily. The dose of chrysin was chosen based on previously reported studies that produced protective effect against reproductive damage [26,27]. On the 14th day, the second and fourth groups were exposed to whole-body irradiation one-hour after vehicle and chrysin administration, respectively. Whole-body irradiation was carried out using a Cesium (^{137}CS) source, Gamma Cell-40 biological irradiator, at the National Center for Radiation Research and Technology (NCRRT), Cairo, Egypt. The animals were exposed to a single dose of 3.2 Gy γ-rays with a dose rate of 0.48 Gy/min. Twenty-four hours after the last chrysin dose, animals were weighed and then; blood samples were collected from the retro-orbital plexus and allowed to clot. Afterward, rats were euthanized via cervical dislocation; ovarian tissues were dissected, washed with ice-cold saline, and then, weighed and stored at −80^{O}C.

2.4. Assessment of relative organ weights

The uteri and ovaries were cleared of connective tissues and weighed. The relative weight of each organ was calculated with relation to final body weight before euthanasia and expressed as mg/100 g body weight.

2.5. Tissue collection and processing

Serum was separated by centrifugation at 5000 rpm for 15 min and kept frozen at -80^{O}C until biochemical assessment of 17β-estradiol (E2) level. Ovarian tissues were homogenized at ratio 1:10 (w/v) in ice-cold 0.1 M phosphate buffer saline (pH 7.4) with an Ultra Turrax homogenizer after that the supernatant was obtained by centrifugation at 10,000 rpm for 15 min then, stored at −80^{O}C until assessment of the levels of TNF-α and TGF-β cytokines. In addition, further ovarian tissues were fixed in an appropriate buffer for light microscopical, electron microscopy as well as immunohistochemical examination of inflammatory markers; NF-κB, iNOS, COX-II, apoptotic markers; cytochrome c and caspase-3, and MAPKs; phosphorylated from of p38 and JNK.

2.6. Histopathological examination

The ovaries of each animal were fixed in 10% neutral buffered paraformaldehyde overnight, then dehydrated in ethanol and embedded in paraffin. To investigate the distribution of ovarian follicles in the ovaries, serial sections of 4 μm thick were deparaffinised with xylene and then, stained with hematoxylin and eosin (H&E) according to standard protocols. Slides were examined and photographed using an Olympus CX21 microscope (Olympus, Japan), and follicles were manually marked and counted.

2.7. Follicle counts

In all ovarian sections, the fifth cut of 4 μm thick was chosen to count the number of follicles per follicle category and to evaluate follicular development across 6 sections using a digital video camera mounted on a light microscope. Follicles were classified as primordial if they contained an oocyte surrounded by flattened pre-granulosa cells, and classified as preantral if they contained an oocyte with a visible nucleus, more than one layer and less than five layers of granulosa cells and lacked an antral space. Follicles were classified as antral if they

contained an oocyte with a visible nucleus, more than five layers of granulosa cells and/or an antral space as described previously [28]. Atretic follicles were identified by the presence of a degenerating oocyte or/granulosa cell's pyknosis [29]. Sum of all follicles demonstrated the ovarian reserve.

2.8. Transmission electron microscopy

Ovarian tissue specimens were immediately fixed in 2.5% phosphate buffered gluteraldehyde (pH 7.4) at 4 °C for 24 h, and post-fixed in 1% osmium tetraoxide for 1 h and then dehydrated by passing them through an ethanol series. After immersion in propylene oxide, specimens were embedded in epoxy resin mixture, and finally sectioned into semi-thin (1-μm-thick) slices. The sections were stained with toluidine blue and examined using a light microscope. Afterward, the tissue blocks were retrimmed and ultrathin (80–90 nm thickness) sections were prepared, collected on copper grids, and stained with uranyl acetate for 15 min and lead citrate for 12 min, examined and photographed using JEOL 1010 transmission electron microscopy (TEM) at Regional Center for Mycology and Biotechnology, Al Azhar University, Cairo, Egypt.

2.9. Biochemical analysis

2.9.1. Assessment of serum estradiol levels

A commercially available ELISA kit was used to measure the circulating level of serum E2 (Monobind Inc., Lake Forest, USA). Quantitative determination of the hormone concentrations was performed according to the manufacturer's protocols. The intra- and inter-assay coefficients of variation were found to be less than 8.2% and 9%, respectively.

2.9.2. Assessment of ovarian tumor necrosis factor (TNF)-α levels

TNF-α was determined in the ovarian supernatant using specific ELISA kits (Assaypro Co, USA) according to the manufacturer's instructions. The intra-assay and inter-assay coefficients of variation were 5.1% and 7.1%, respectively. The TNF-a levels were presented as ng/g tissue.

2.9.3. Assessment of ovarian transforming growth factor (TGF)-β levels

TGF-β level of ovarian tissue was determined in the supernatant by using commercial ELISA kit (Cusabio Biotech Co., Wuhan, China) in accordance with the protocol specified by the manufacturer. The intra-assay and inter-assay coefficients of variation were 8% and 10%, respectively. The TGF-β levels were presented as ng/g tissue.

2.10. Immunohistochemistry of ovarian NF-κB, iNOS, COX-II, cytochrome c, caspase-3, phospho- p38, and phospho- JNK

Sections were stained using a fully automated immunohistochemistry device. Paraffin embedded ovarian tissue sections of 3 μm thick were dehydrated first in xylene and next in graded ethanol solutions. The slides were then blocked with 5% bovine serum albumin in Tris buffered saline for 2 h. Then, IHC staining was performed by a standard streptavidin-biotin-peroxidase procedure. The sections were incubated with a rabbit polyclonal antibody to rat nuclear factor kappa b (NF-kB), (Thermo Fisher Scientific, Cat. No. RB-9034-P); inducible nitric oxide synthase (iNOS), (Thermo Fisher Scientific, Cat. No. RB-9242-P); cyclooxygenase (COX)-2, (Thermo Fisher Scientific, Cat. No. RB-9072-R7); caspase-3 (Thermo Fisher Scientific, Cat. No. PA5-77887); a mouse monoclonal antibody to rat cytochrome c (Thermo Fisher Scientific, Cat. No. MS-1192-R7); rabbit polyclonal antibody to rat phospho-JNK (R& D systems, Cat. No. AF1205), or p38 (R& D systems, Cat. No. AF869), overnight at 4^{O}C. After rinsing thoroughly with Tris buffered saline, the sections were incubated with a biotinylated goat anti-rabbit secondary antibody, after that, the horseradish-peroxidase-conjugated streptavidin solution was added and incubated at room temperature for 10–15 min. Finally, the sections were visualized with 3,3′-diaminobenzidine containing 0.01% H_2O_2. Counter staining was performed using hematoxylin, and the slides were visualized under a light microscope. The slides were processed immunohistochemically at the same laboratory conditions in order to obtain comparable staining intensities. The digital colour images were registered using a light microscope (CX21,OLYMPUS, JAPAN) equipped with a camera AxioCam HRc (Carl Zeiss, Jena, Germany) and connected to a computer. Then, the immunohistochemical quantification was carried out by measuring optical density in 7 high power fields of at least five rat ovaries using image analysis software (Image J, 1.46a, NIH, USA).

2.11. Data analysis

Continuous variables are presented as the mean ± SD and were analyzed by one-way analysis of variance (ANOVA) followed by Tukey–Kramer as a post-hoc test. Moreover, the number of ovarian follicles was compared using Kruskal-Wallis's test followed by Dunn's multiple comparisons as a post-hoc test. The probability level less than 0.05 was considered to indicate statistical significance. All statistical analyses were performed using Instat version 3 software package. Graphs were sketched using GraphPad Prism version 5 software (GraphPad Software Inc., USA).

3. Results

3.1. Ovarian and uterine weights

Female rats exposed to γ-radiation showed significant reduction in ovarian and uterine weights by 20% and 33%, respectively as compared to control group. On the other hand, chrysin treatment significantly counteracted these effects and maintained ovarian and uterine weights comparable to that of the control group. Animals treated with chrysin alone did not show any significant differences in sex organs weights as compared with the control group (Table 1).

3.2. Circulating estradiol level

The impaired reproductive capacity in the irradiated female rats was confirmed by a drastic decrease in serum E2 levels by 26% as compared to the control group (151.58 ± 21.74 vs. 205.33 ± 12.00 in control). Notably, compared to vehicle-treated irradiated group, chrysin administration significantly increased the circulating E2 levels by 75% in the irradiated rats (264.72 ± 44.24 vs. 151.58 ± 21.74) restoring their levels to that of the control group. Chrysin treatment alone did not show any significant difference in serum E2 levels as compared to the control group (Fig. 1 **panel A**).

Table 1
Effect of chrysin administration (50 mg/kg, P.O.) on *Y*-radiation-induced ovarian, and uterine weight loss.

	Relative ovarian weight (mg/100 g Body weight)	Relative uterine weight (mg/100 g Body weight)
Control	54.85 ± 7.43	124.80 ± 26.72
IR	44.09 ± 5.18*	83.60 ± 14.58*
Chrysin	53.86 ± 8.05#	125.92 ± 32.76#
Chrysin/IR	54.40 ± 7.05#	120.04 ± 38.76#

Data expressed as mean ± SD (N = 12). Statistical analysis was done using ANOVA followed by Tukey–Kramer as a post hoc test.
* $p < 0.05$ compared to control group.
# $p < 0.05$ compared to irradiated (IR) group.

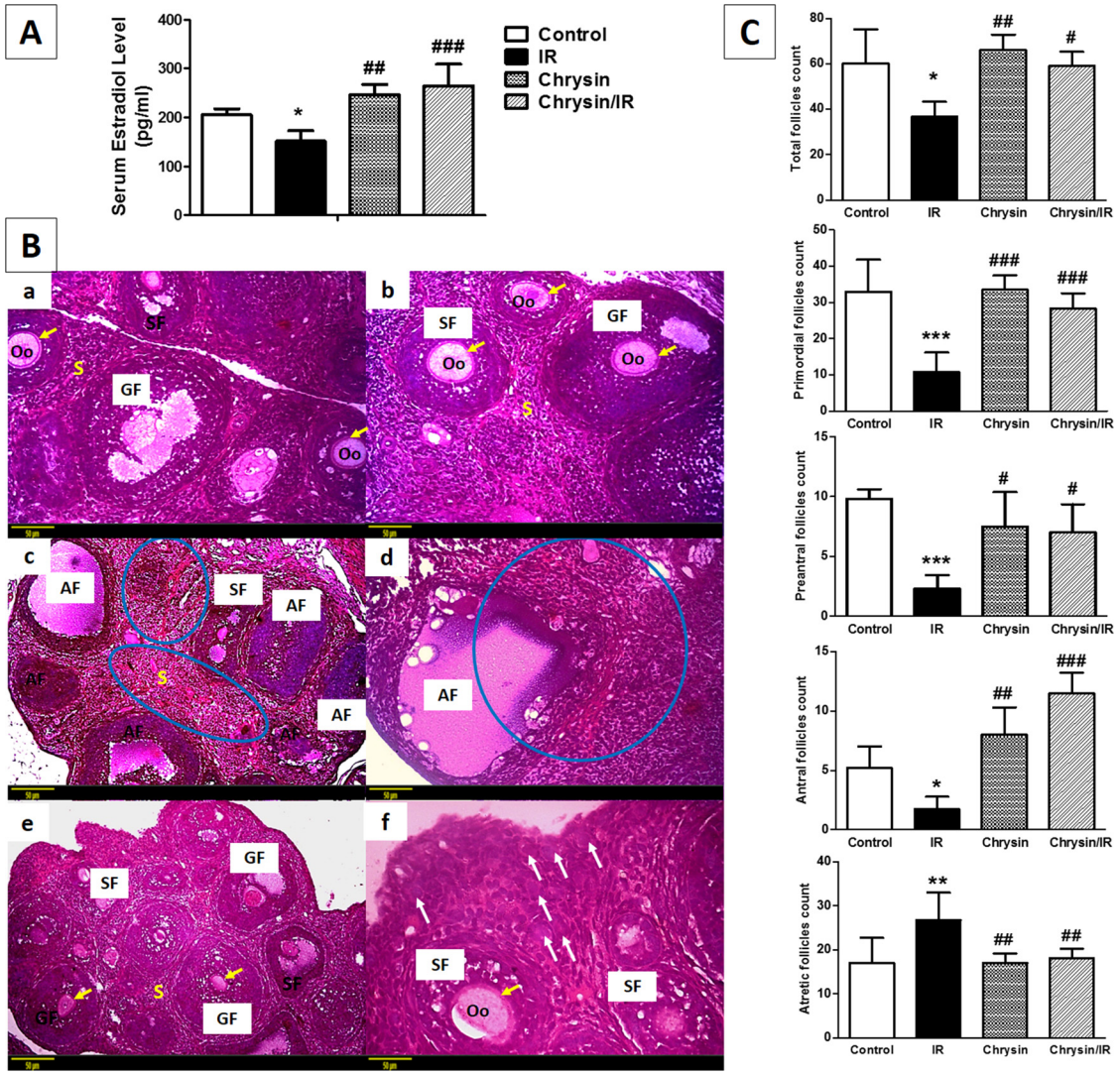

Fig. 1. Serum estradiol levels and ovarian follicles' assembly.

Panel A: Changes in serum estradiol levels of female rats subjected or not to ϒ-radiation and/or chrysin treatment. Values are given as mean ± SD (N = 10). Statistically significant differences were assessed using one-way ANOVA followed by Tukey–Kramer as a post hoc test. * $p < 0.05$ compared to control group, $^{\#\#}$, $^{\#\#\#}$ indicate $p < 0.01$ and $p < 0.001$ compared to irradiated (IR) group. **Panel B:** Photomicrographs illustrating the effect of chrysin treatment and/or radiation exposure on the histological architecture of the ovary (using hematoxylin and eosin staining). Normal oocyte (Oo) and zona pellucida (yellow arrow) structure in control (a) and chrysin (b) groups with different stages of follicle development could be seen with normal-looking follicles. Many atretic follicles (AF), congested blood vessel, interstitial hyperplasia, vacuolization, as well as marked fibrosis (blue circle) can be seen in the radiation-only group (c&d). Treatment with chrysin improved these changes as shown by an apparent normal zona pellucida (yellow arrow) structure, numerous healthy primordial (white arrow), secondary (SF), and graafian (GF) follicles (e&f). Scale bar, 50 µm. **Panel C:** Morphometric analysis of ovarian primordial, preantral, antral, and atretic follicle populations. The mean ± SD from a minimum of five different rat ovaries was performed. Statistically significant differences were assessed by Kruskal–Wallis's test followed by Dunn's multiple comparisons as a post hoc test. *, **, *** indicate $p < 0.05$, $p < 0.01$ and $p < 0.001$ compared to control group, $^{\#}$, $^{\#\#}$, $^{\#\#\#}$ indicate $p < 0.05$, $p < 0.01$ and $p < 0.001$ compared to irradiated (IR) group. SF, secondary follicle; GF, graafian follicle; AF, atretic follicle; Oo, oocyte.

3.3. Histopathological and morphological findings

The control and chrysin only treated groups showed normal ovarian morphological architecture of cortical and medullary portions with different stages of follicle development **(**Fig. 1 **panel B: a&b)**. However, in the radiation group, almost all of the follicles were atretic and no primordial follicles were observed **(**Fig. 1 **panel B: c)**. Also, the granulosa layer in the atretic follicles was found to be loosened generally. Growing follicles had relatively irregular arrangements with a discrete theca layer and also uneven thickness of the zona pellucida layer in some parts of the follicles. Most of the primary follicles were found to lack oocytes, and the structure of the ovarian stroma was disrupted. Also, vascular congestion, hemorrhage, and accumulation of collagen fibers in the form of fibrosis were detected in the stroma **(**Fig. 1 **panel B: d)**. In contrast to the radiation group, the primary, secondary, and graffian stages follicles were observed, and numerous normally-looking primordial follicles were also detected in the irradiated group co-treated with chrysin **(**Fig. 1 **panel B: e&f)**. In addition, administration of chrysin preserved ovarian tissue from radiation-induced hemorrhage and fibrosis.

Next, we inquired which stages of follicular development were impacted in different treatment groups. To this end, the population of primordial, growing, and atretic follicles of different cohorts was determined. Follicle counts of each group are given in Fig. 1**C**. There was a statistically significant difference in follicle counts (primordial, preantral, antral, and atretic follicles) between studied groups. Sections of control ovaries had a total of 60.25 ± 14.88 follicles that were distributed among primordial follicles, 33.00 ± 8.81; preantral follicles,

9.80 ± 0.84; antral follicles, 5.20 ± 1.81; and atretic follicles, 17.00 ± 5.76. The total number of follicles was drastically decreased by 40% after exposure to *Y*-radiation as compared to control ovaries. The population of primordial, preantral, and antral follicles was significantly reduced by 65%, 80%, and 60%, respectively in irradiated ovaries as compared to the control group. Conversely, the number of atretic follicles significantly increased in the irradiated ovaries by 53% as compared to the control group. Interestingly, irradiated rats treated with chrysin showed significant increase in the population of primordial, preantral, and antral follicles, and significant decrease in the number of atretic follicles as compared to the irradiated group. There was no statistically significant difference in the count of different follicles population between the control and chrysin only treated groups.

3.4. Electron microscopy

TEM was used to detect the ovarian tissue ultramicrostructure of different treatment groups. Oocyte from control group and chrysin alone treated group have intact cell membranes, normal mitochondrial cristae distributed among cytoplasm and Golgi complexes, and clear nuclei with normal morphology. Moreover, zona pellucida, located between the oocyte and granulosa cells, had a uniform thickness, and presence of cilia attached it to oocyte plasma membrane **(**Fig. 2**A & C)**. Additionally, control and chrysin treatment alone showed normal granulosa cells structure observed with normal nucleus and chromatin granules which were homogeneously dispersed throughout the nuclei as visualized by TEM and the tight junction between granulosa cells (Fig. 2 **B&D**).

On the other hand, Fig. 2 **(E&F)** shows the ultrastructural pathological changes in ovarian oocyte and granulosa cells after γ-radiation exposure. Strikingly, the oocytes were devoid of their nucleus, mitochondria and Golgi apparatus. Moreover, zona pellucida showed very thin thickness. The granulosa cells of irradiated ovaries were severely degeneration as evident by the abnormal nucleus, irregular nuclear membrane with condensed and un-uniform chromatin, and absence of Golgi apparatus. Swollen mitochondria with decreased mitochondrial cristae as well as lipid droplets and autophagosomes were clearly visible in the electron micrograph. In addition, fibrous tissue in between the granulosa cells (polygonal cell) and theca cells (flattened cell) was obvious.

Chrysin treatment protected the oocytes and granulosa cells from the damaging effects of radiation (Fig. 2 **G&H**), as it preserved the normal oocyte and granulosa cell structure as evidenced by the presence of nucleus with normal chromatin distribution, multiple golgi apparatus and normal mitochondria cristae distributed among the cytoplasm, presence of oocyte plasma membrane attached to zona pellucida via cilia. Granulosa cells (polygonal cells) returned attached to each other through the tight junction between them as they were loose in irradiated ovaries. However, some granulosa cells converted to neutophils (Nu) and phagocytic cells (P) which are normal looking granulosa cells. Furthermore, irradiated group treated with chrysin showed that the ovarian ultrastructure was devoid of granulosa cells infiltrating the oocyte, fibrous tissues either inside or outside oocyte, and fatty droplets and autophagosomes that - in contrast - were evident in irradiated ovaries.

3.5. Inflammatory markers

As a key inflammatory cytokine, TNF-α was assessed by measuring its ovarian tissue content using ELISA. The ovarian TNF-α level was significantly higher in the ovaries of irradiated rats by 28% as compared with controls (0.86 ± 0.06 versus 0.67 ± 0.07). Conversely, chrysin treatment significantly inhibited the elevation of TNF-α levels in irradiated rats and kept it close to that of controls. For the non-irradiated rats, the level of TNF-α showed no change after chrysin treatment as compared to the control levels (Fig. 3A).

The inflammatory responses provoked by radiation were further assessed by measuring the expression of NF-kB p65 COX-2, and iNOS proteins using immunohistochemistry. Immunohistochemical staining of NF-kB p65 revealed that ovarian sections of control and chrysin treated alone showed a mild degree of immunostaining for NF-kB p65. Irradiated ovaries showed an increase in the NF-kB p65 immunoreactivity in the cytoplasm of follicular oocyte, granulosa and theca cells, as well as ovarian stromal cells, which was evident by

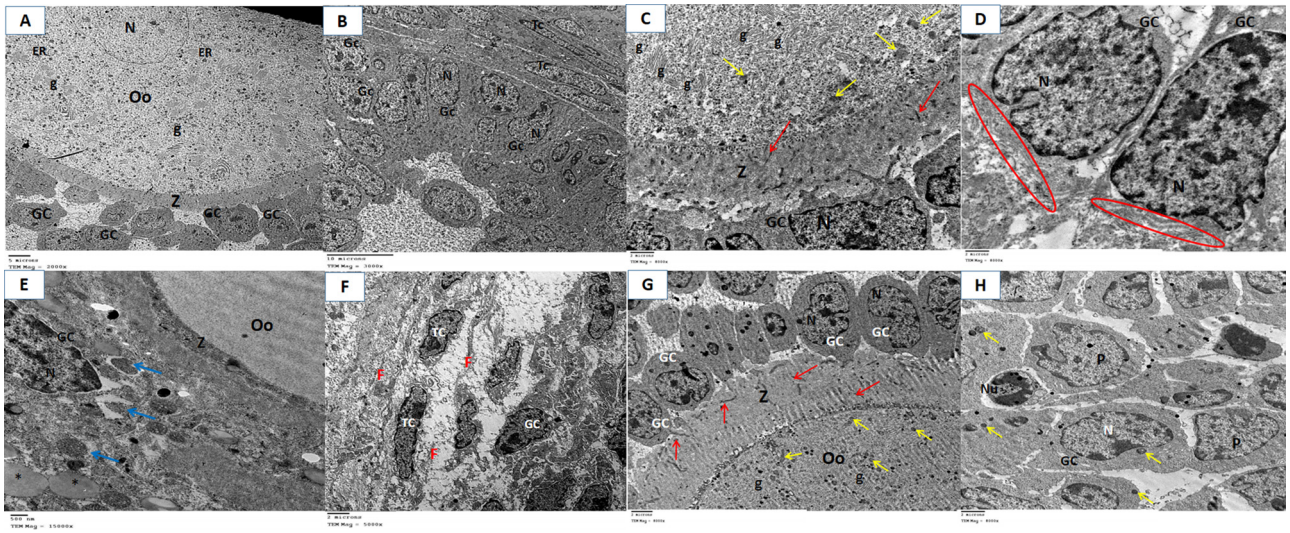

Fig. 2. Ultrastructural views of normal and altered ovarian follicles of different treatment groups.
Ultrathin sections of control **(A&B)** and chrysin-only treated ovaries **(C&D)** represent normal oocyte (Oo) and granulosa cells (GC) structure with normal nucleus (N), and numerous mitochondrial cristae (yellow arrow). Oocyte cytoplasm contains Golgi complexes (g), rough endoplasmic reticulum (ER). Zona pellucida (Z) had a uniform thickness and a homogeneous density with visible oocyte cytoplasmic cilia (red arrow). Also, gap junction between granulosa cells is obvious (red circle). **(E &F)** Ultrathin sections of ovaries of radiation exposed rats showed absence of golgi apparatus and mitochondria from oocyte cytoplasm. Zona pellucida (Z) showed very thin thickness. Granulosa cells of irradiated ovaries were loose from each other with abnormal nucleus and condensed chromatin. Lipid droplets (*), autophagosomes (blue arrows), and fibrous tissue in between granulosa cells (GC) and theca cells (TC) were clearly visible. **(G&H)** Ultrathin sections of chrysin/irradiated ovaries showed normal oocyte and granulosa cell structure. Some granulosa cells converted to neutophils (Nu) and phagocytic cells (P).

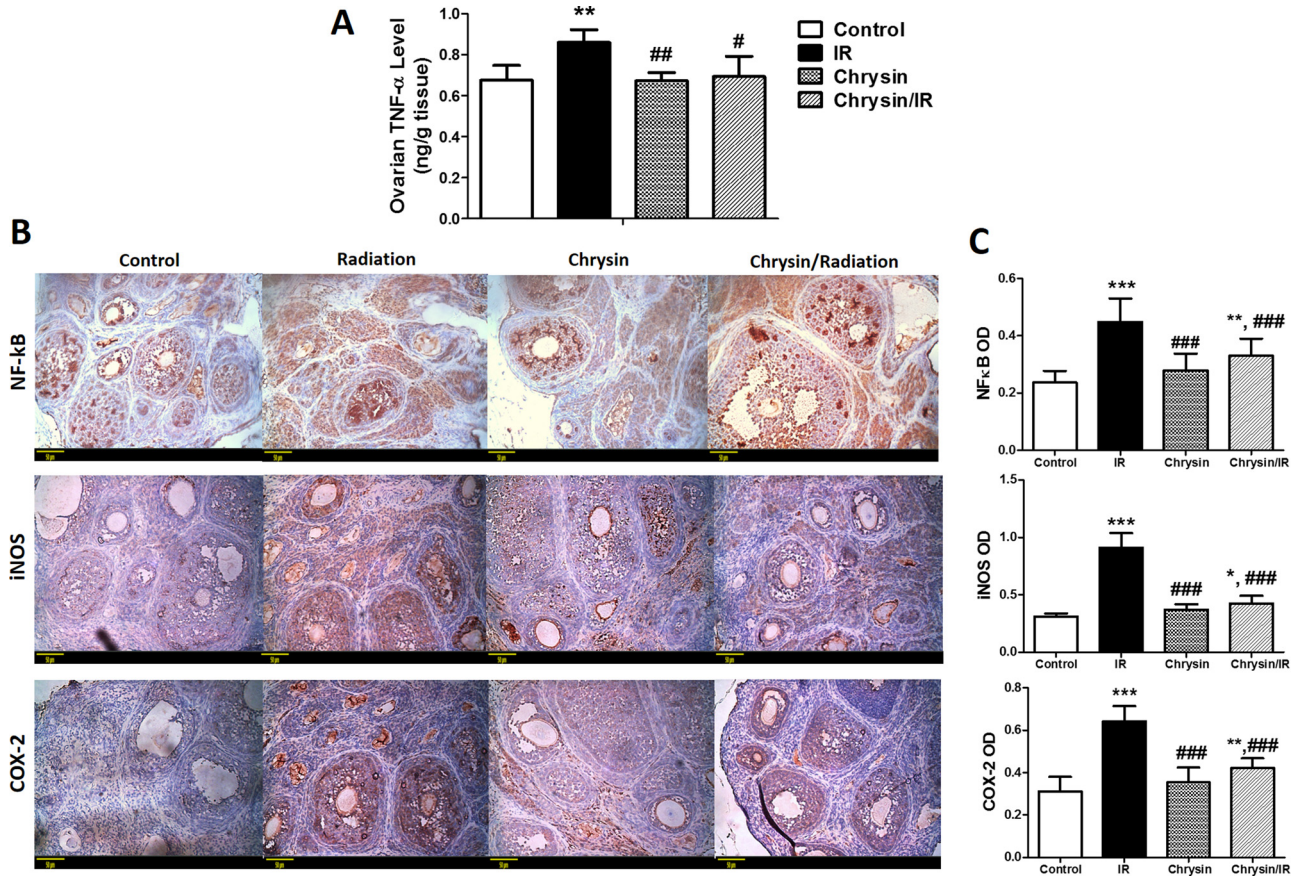

Fig. 3. Chrysin downregulates inflammatory signaling pathway boosted in radiation-induced ovarian injury.

Panel A: The levels of cytokine TNF-α in ovarian tissues of immature rats were determined using ELISA. Values are given as mean ± SD (n = 6). Statistically significant differences were assessed using one-way ANOVA followed by Tukey–Kramer as a post hoc test. ** $p < 0.01$ compared to control group, $^{\#}$, $^{\#\#}$ indicate $p < 0.05$ and $p < 0.01$ compared to irradiated (IR) group.

Panel B: Cellular localization of NF-kB, iNOS, and COX-2 proteins in the ovaries obtained from ϒ-radiation exposure and/or chrysin treated immature rats. Ovarian sections of control and chrysin-only treated rats show a minimal degree of NF-kB, iNOS and COX-2 expression in follicle oocyte, as well as granulosa, theca, and interstitial cells. Note the greater levels of NF-kB immunoreactivity (intense brown staining) in granulosa and interstitial cells, as well as marked immunoreactivity of iNOS and COX-2 enzymes in the cytoplasm of follicle' oocytes and granulosa cells of irradiated rats. In contrast, treatment with chrysin showed minimal immunoreactivity to NF-kB and negative oocyte and granulosa cells' cytoplasmic expression of iNOS and COX-2. Scale bar, 50 µm.

Panel C: Quantitative analysis of NF-kB, iNOS, and COX-2 staining intensity in the ovaries of female rats in experimental groups expressed as optical density (OD) of immunopositive cells averaged across 7 fields for each rat section. Each column represents the mean ± SD of at least five rat ovaries. Statistically significant differences were assessed using one-way ANOVA followed by Tukey–Kramer as a post hoc test. *, **, *** indicate $p < 0.05$, $p < 0.01$ and $p < 0.001$ compared to control group, $^{\#\#\#}$ $p < 0.001$ compared to irradiated (IR) group.

strong positive brown staining. In contrast, chrysin treatment showed moderate NF-kB immunoreactivity of the granulosa cells indicating a significant down-regulation of NF-kB p65 expression in comparison to irradiated ovaries (Fig. 3**B; 1st row**). The immunohistochemical staining was quantified and the optical density of NF-kB p65 immunopositive cells of the irradiated ovaries treated with chrysin was dramatically decreased by 27% compared to that of the irradiated ovaries (Fig. 3C).

In addition, immunohistochemical detection of proinflammatory enzymes iNOS and COX-2 revealed that the ovaries of the control and chrysin only treated rats showed minimal expression of both enzymes (Fig. 3B**, 2nd and 3rd rows**). In contrast, radiation-exposed ovarian tissue displayed marked elevation of iNOS and COX-2 immunoreactivity predominantly localized in the granulosa cells and theca of the ovary. Rats treated with chrysin showed moderate iNOS and COX-2 immunoreactivity of the granulosa and theca cells compared to the radiation-exposed ovary. Optical density analysis of these proinflammatory enzymes' immunoreactivity was performed using the image J analysis software, and the results are represented in Fig. 3**C**.

3.6. Apoptotic markers

The effects of radiation on the mitochondrial- dependent apoptotic pathway was examined by determination of protein expression of both cytochrome c and caspase-3 enzyme using immunohistochemical technique (Fig. 4 **A&B**). Both control and chrysin only-treated groups were minimally stained for both apoptotic markers. Cytochrome c and caspase- 3 were expressed mainly in the granulosa cells of atretic follicles. Their expression was absent in the granulosa cells of healthy follicles. Contrariwise, radiation caused a marked increase in the expression of both cytochrome c and caspase 3 proteins in the ovarian granulosa and theca cells as well as interstitial cells which was evident from the intensive brown color. While treatment of irradiated animals with chrysin reduced this elevated expression as compared to irradiated group as manifested by fainter brown staining. The immunohistochemical staining was quantified as optical density of the stained regions using the image J analysis software, and the results are represented in Fig. 4 **C**.

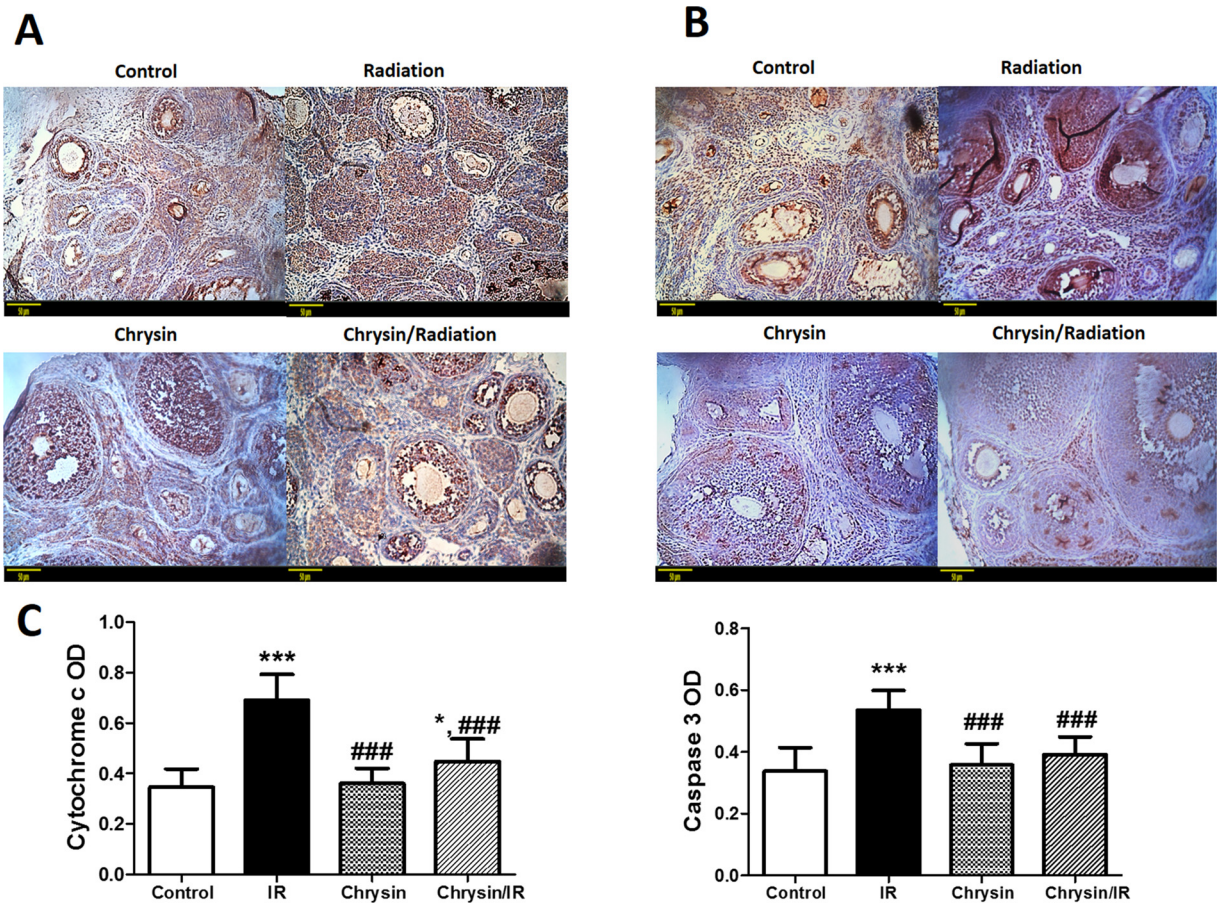

Fig. 4. Chrysin opposes γ-radiation induced ovarian apoptotic cell death.
Cellular localization of cytochrome c **(Panel A)** and caspase-3 **(Panel B)** proteins in the ovaries obtained from *Y*-radiation exposure and/or chrysin treated immature rats. Expression of cytochrome c and caspase-3 proteins was weakly detected in the control and chrysin-only treated group's ovary. Marked immunoreactivity of cytochrome c and caspase-3 in the ovary of *Y*-radiation exposed rats was detected mainly in granulosa and interstitial cells. Moderate immunoreactivity of cytochrome c and caspase-3 proteins in chrysin pretreatment irradiated rats. Scale bar, 50 μm.
Panel C: Quantitative analysis of cytochrome c and caspase-3 staining intensity in the ovaries of female rats in experimental groups expressed as optical density (OD) of immunopositive cells averaged across 7 fields for each rat section. Each column represents the mean ± SD of at least five rat ovaries. Statistically significant differences were assessed using one-way ANOVA followed by Tukey–Kramer as a post hoc test. *, *** indicate $p < 0.05$ and $p < 0.001$ compared to control group, $^{###}$ $p < 0.001$ compared to irradiated (IR) group.

3.7. TGF-β/p38/JNK signaling pathway

To further explore the molecular mechanisms associated with radiation-induced ovarian injury, the role of TGF-β/ MAPK signaling pathways was investigated in the ovarian tissues via measuring the protein expression of TGF-β cytokine and the phosphorylated forms of both p38 and JNK proteins. The levels of TGF-β cytokine was significantly higher in the ovaries of irradiated rats by 225% when compared with the control (1.11 ± 0.22 *vs* 0.33 ± 0.09). In contrast, treatment of irradiated rats with chrysin prevented the elevation of TGF-β and retained it close to that of controls. No significant change was observed in the ovarian TGF-β l in the control and non-irradiated rats treated with chrysin (Fig. 5A).

Regarding MAPKs, immunohistochemical examination of the phosphorylated forms of both p38 and JNK respectively revealed minimal expression of both proteins in both control and chrysin alone-treated groups (Fig. 5B). On the other side, radiation induced activation of both p38 and JNK as evidenced by the markedly elevated expression of the phosphorylated forms of both proteins. Interestingly, chrysin treatment effectively hindered the activation of MAPKs as shown by the apparent reduction in the expression of phosphorylated protein of both p38 and JNK as compared to the radiation group (Fig. 5B). The immunohistochemical staining was quantified as optical density of the stained regions using the image analysis software, and the results are represented in Fig. 5**C**.

4. Discussion

Preservation of fertility has become increasingly important in improving the quality of life of completely recovered cancer patients. Pharmacological protective adjuvants that can protect the dormant ovarian follicle pool and prevent follicle loss during radiotherapy is highly effective strategy for preserving female fertility and poses less of a burden on the human body [30]. Interestingly, side by side with the well-established anticancer activities of chrysin, its radioprotective effects have been reported in different models of toxicities [19,24,25]. However, the potential ameliorative effect of chrysin in ovarian development and radiation biology remain elusive. Therefore, this study investigated the potential protective effects of chrysin on radiation induced-ovarian damage and elucidated the underlying molecular mechanisms.

In our study, the ovarian function was significantly impaired following its exposure to a single dose of γ-radiation which was characterized by markedly-reduction of ovarian folliculogenesis and endocrine function. Regarding the hormonal status, ovarian failure is manifested as hypergonadotropic hypogonadism [31]. It is interesting

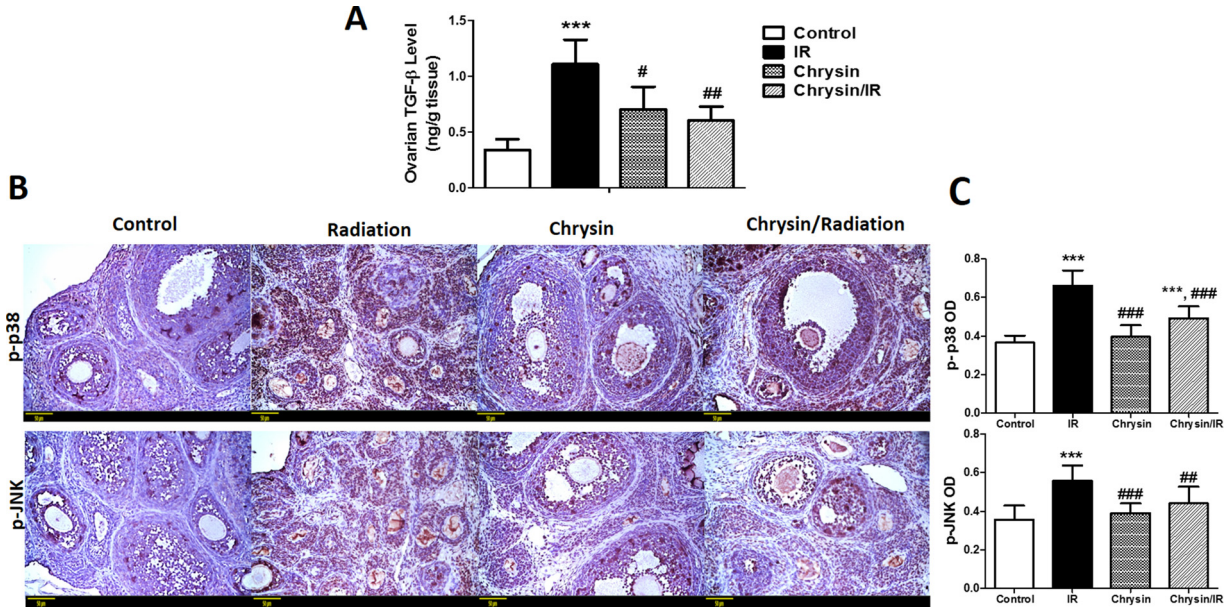

Fig. 5. Chrysin downregulates TGF-β/MAPK pathway in ovaries of irradiated rats.

Panel A: ELISA assay of ovarian TGF-β levels. Values are given as mean ± SD (n = 6). Statistically significant differences were assessed by a one-way ANOVA followed by Tukey–Kramer as a post hoc test. *** $p < 0.001$ compared to control group, $^{\#}$, $^{\#\#}$ indicate $p < 0.05$ and $p < 0.01$ compared to irradiated (IR) group.

Panel B: Cellular localization of p-p38 and p-JNK MAPKs in rat ovaries. Positive staining was observed in oocytes and granulosa cells. Expression of p-p38 and p-JNK proteins was weakly detected in the ovaries of control and chrysin-only treated groups. Radiation increased the phosphorylation of p38 and JNK MAPKs in the ovary as detected by intense brown staining. Downregulation of p-p38 and p-JNK was observed in chrysin/radiation treated group when compared to radiation-exposed rats. Scale bar, 50 μm.

Panel C: The expression of the corresponding protein in the ovaries of different experimental groups are expressed as optical density (OD) of immunopositive cells averaged across 7 fields for each rat section. Each column represents the mean ± SD of at least five rat ovaries. Statistically significant differences were assessed using one-way ANOVA followed by Tukey–Kramer as a post hoc test. *** $p < 0.001$ compared to control group, $^{\#\#}$, $^{\#\#\#}$ indicate $p < 0.01$ and $p < 0.001$ compared to irradiated (IR) group.

that serum E2, but not FSH, is important as a predictive factor for the follicular development, as indicated in the multivariate analysis [32]. Our result confirmed the previous one which reported a drop in serum E2 levels 24 h after radiation exposure [33]. Since estrogen is synthesized and secreted by growing follicles, the observed decrease in E2 concentrations in the irradiated group may be partly attributable to the profound toxicity imposed on the follicular ovarian reserve and function [33]. On the other hand, chrysin administration completely-prevented the decrease in E2 level induced by irradiation.

Moreover, while the exposure to a single dose of γ-radiation negatively affected the ovary weight, chrysin treatment reversed such effects preserving the normal "control" phenotype. In this context, the number of follicles, especially quiescent primordial follicles, is a more direct parameter whose assessment allows an accurate estimation of ovarian reserve. The ovary is highly sensitive to γ-radiation which destroys follicles at all stages of growth; however, primordial stage follicles appear to be most sensitive [34]. Primordial follicles provide the reserve for the production of growing follicles and ova over a prolonged period of time and once its reserve is depleted, ovarian failure ensues. In the present study, histopathological examination showed that γ-radiation dramatically depleted the reserve of primordial follicles as well as growing pre-antral and antral follicles within a time period of four days. Our finding is consistent with the hypothesis that ionizing radiation leads to follicular depletion by damaging rapidly dividing granulosa cells. This consequently lead to a decrease in gonadal steroid secretion which stimulates a negative feedback enhancing the recruitment of primordial follicles into the pool of growing follicles resulting in the depletion of primordial follicles and eventually POF [35]. These findings were further confirmed by the results of the electron microscopic examination of the ovarian tissues which displayed some abnormal ultrastructural alterations in the ovarian mitochondria such as swelling, cristae disorder, and vacuolation upon γ-radiation exposure.

Interestingly, chrysin treatment remarkably preserved primordial follicles' stock, minimized the follicle depletion induced by γ-radiation, and counteracted γ-radiation-induced pathological ovarian ultrastructural alterations. Collectively, hormonal, histopathological and ultramicrostructure examinations verified the potent capability of chrysin administration to prevent radiation-induced POF. Consequently, the next aim of our study was to explore the molecular mechanisms underlying these potential radioprotective effects of chrysin against ovarian follicles depletion.

The apoptotic events have been reported to play a key role in radiation-induced ovarian damage [33,36]. Ionizing radiation triggers the intrinsic apoptotic pathway which is characterized by destruction of the mitochondrial membrane that contributes to the release of cytochrome c from the mitochondria to the cytosol [37]. Then, a cascade of reactions occurs, which includes cytochrome binding with Apaf-1 resulting in the activation of the initiator caspase 9 and triggering the activation of the effector caspase 3 [38]. Theoretically, radiotherapy targets actively dividing cells. Therefore, the logical targets for radiotherapy are not dormant, mitotically inactive cells, but rather the proliferating cells around growing or mature follicles. Consistently, irradiation did not induce primordial follicle apoptosis in our study. Indeed, while the population of primordial follicles decreased without any indications of increased apoptosis, prominent apoptotic features were prevalent among the primary and secondary follicles as evidenced by the elevated expression of apoptotic markers cytochrome c and caspase 3 in ovarian granulosa and theca cells. Considering that POF is characterized by sex steroid deficiency, E2 is a major determinant of follicle development and decreases granulosa cell apoptosis in rodents. Consequently, in our study, irradiation-induced ovarian follicles atresia might be secondary to reduced E2 levels which in turn predispose cells to apoptosis. Notably, this was counteracted by the antiapoptotic bioactivities of chrysin which are reported to contribute to its beneficial effects

guarding against many toxicities [39,40].

Another critical pathway which significantly contributes to the ovarian follicular loss upon exposure to radiation is the inflammatory signaling pathway [8]. Normally, unperturbed inflammation plays a key physiologic role in appropriate folliculogenesis and ovulation. However, increasing evidence has demonstrated that aberrant inflammation can alter normal ovarian follicular dynamics contributing to infertility [7]. The temporal changes in the ovary which appear to resemble inflammation first led to the concept that ovulation is reminiscent of an inflammatory response. Electron microscopy in our study monitored the morphological changes in the ovary during follicular development and demonstrated a significant rearrangement of connective tissue and fibroblast activation. Accumulating evidence has indicated that the transcription factor NF-kB, the master regulator of the transcription of many inflammatory genes, plays pivotal roles in the ovarian tissue inflammation induced by various damaging insults such as chemotherapy, ischemia repefursion injury, or radiation associated ovarian injury [8,41–43]. In this context, NF-kB activation following radiation exposure represents a key element in the radiation- induced inflammatory responses [44,45], where the transcription of a cluster of NF-κB regulated cytokines, including TNF-α is upregulated hence contributing to radiation-induced tissue damage [46].

Besides boosting the cytokines expression, NF-kB also induces the expression of many inflammatory enzymes including COX-2 and iNOS [47], which further contributes to follicular atresia induced by radiation. Overexpression of COX-2, due to inflammation, could be deleterious to the female reproductive organs. Apart from this, iNOS is stimulated by the pro-inflammatory cytokine TNF-α to increase the level of NO which induces ovarian toxicity [48]. In the current study, γ-radiation elicits potent inflammatory responses as shown by the elevated protein expressions of the inflammatory markers; NF-kB, TNF-α, COX II, and iNOS in the ovaries of the irradiated rats. Seriously, follicular atresia present in ovarian function injury is associated with an inflammatory response [49]. Conversely, chrysin administration effectively abolished these inflammatory reactions as shown by the marked reduction in all inflammatory proteins. These findings are in agreement with previous ones reporting the promising anti-inflammatroy properties of chrysin which are mainly mediated by suppressing NF-kB expression and hence the downstream inflammatory signals [20,50].

Taken together, our previous findings pointed out that chrysin could effectively abrogate radiation-induced ovarian injury via suppressing both inflammatory and apoptotic events. In this regard, various molecular mechanisms are implicated in regulating both processes, one of these critical mechanisms is TGF-β signaling pathway. TGF-β1 is a member of TGF-β super family of cytokines, which functions in growth, development, immunity, wound healing, inflammation, apoptosis, and cancer [51]. Certain TGF-β family members affect the control of granulosa cell growth and differentiation [52]. In addition, TGF-β superfamily is vital for steroidogenesis process in granulosa cells [53].

Despite the lack of data demonstrating the role of TGF-β isoforms in oocyte endowment or primordial follicle assembly and activation, there is evidence supporting the inhibitory role of TGF-β in preantral follicle growth that most likely involves an increase in apoptosis at the primary and preantral stages of the follicle development [54]. In addition, TGF-β has been implicated in the development of radiation-induced toxicities in several organs including the skin, lung, and liver [6,55]. Upon its activation, binding of TGF-β1 to its receptor triggers signals mediated by the phosphorylation and activation of Smad2 and Smad3. Then, Smad4 binds activated Smad2/3, and translocates into the nucleus to regulate the transcription of related genes [56].

In addition to the Smad-mediated canonical TGF-β signaling pathway, several lines of evidence reported that TGF-β may signal through other pathways. The mitogen-activated protein kinases (MAPKs) are one of the non-Smad pathways representing a key signal transduction pathway in regulating both inflammatory and apoptotic processes [57]. Curiously, crosstalk between TGF-β and MAPK pathways is involved in mediating the biological effects of ionizing radiation. MAPKs are serine-threonine kinases which consist of extracellular signal-regulated kinase (ERK), p38 mitogen-activated protein kinase (p38), and c-Jun N-terminal kinase (JNK) [58]. They are activated by diverse extracellular and intracellular stimuli including peptide growth factors, cytokines, hormones, and various cellular stressors such as oxidative stress [59]. Activation of MAPKs is mediated by upstream phosphorylations via MAPK kinases. Once activated, MAPKs regulate the expression of various genes involved in the regulation of many cellular processes including cell growth, differentiation, and apoptosis [60]. In this regard, MAPK signaling pathways positively regulate the transcription of several inflammatory genes, such as those coding for TNF-α, IL-1β, and COX-2 enzyme [61]. In addition, compelling evidence indicated that both p38 and JNK kinases contribute to the activation of the transcription factor NF-kB by promoting the degradation of its inhibitory protein; IkBα [62]. Furthermore, the pro-inflammatory cytokine TNF-α upon binding to its receptors induces the activation of both MAPKs and NF-kB signal pathways leading subsequently to an amplification loop of inflammatory signals inducing further tissue damage [63].

Beside their effects on inflammatory cascades, MAPK have crucial roles in signal transduction of apoptotic cell death [64]. This is attributed to activating some mitochondrial-associated factor (e.g., Bax) which is a pro-apoptotic protein leads to initiation of intrinsic pathway of apoptosis hence release of cytochrome c from injured mitochondria and finally caspase activation. Indeed, it was reported that p38 and JNK are activated during apoptotic death of the granulosa cells of preovulatory follicles [65]. Besides both kinases were also reported to be associated with apoptosis of small preantral ovarian follicles caused by 4-vinylcyclohexene diepoxide intoxication in rats [66].

In consistent with the aforementioned studies, the current study stated that exposure to radiation induced activation of TGF-β signaling pathway as shown by the markedly elevated levels of TGF-β in the ovarian tissues of irradiated rats. Consequently, TGF-β activation elicited activation of the downstream MAPKs as evidenced by the increased expressions of phosphorylated forms of p38 and JNK proteins. In agreement with our findings, there is substantial evidence supporting the importance of TGF-β in boosting the inflammatory responses and subsequently developing excessive fibrosis following the exposure to radiation in animals and humans [67,68]. Moreover, both p38 and JNK have been reported to be involved in radiation-induced mitochondrial dysfunction and apoptotic cell death [69]. Notably, chrysin administration effectively blunted the radiation-induced activation of TGF-β signaling pathway as it abolished the elevated levels of TGF-β cytokine and the phosphorylated forms of both p38 and JNK proteins. Our results are in consistent with previous one which reported that chrysin effectively guarded against isoproterenol-myocardial injury in rats via suppressing TGF-β signalling and the downstream MAPKs; p38 & JNK [22].

Collectively, this study provides an evidence for the first time for the cytoprotective effects of chrysin against radiation-induced ovarian damage. Mechanistically, TGF-β/MAPK signaling emerges as a new therapeutic target implicated in mediating radiation-induced POF. The potent anti-inflammatory and anti-apoptotic effects of chrysin can be attributed to its inhibitory effects on TGF-β signaling pathway and the downstream MAPK cascades. Hopefully, our data provides therapeutic rationale for using chrysin as an adjuvant therapy to promote the repair and recovery of ovarian function in POF cancer patients following radiotherapy.

Declarations of interest

None.

Funding

This research did not receive any specific grant from any funding

agencies in the public, commercial, or not-for-profit sectors.

References

[1] M. Plummer, C. de Martel, J. Vignat, J. Ferlay, F. Bray, S. Franceschi, Global burden of cancers attributable to infections in 2012: a synthetic analysis, Lancet Glob. Heal. 4 (2016) e609–e616, https://doi.org/10.1016/S2214-109X(16)30143-7.

[2] M. Najafi, A. Shirazi, E. Motevaseli, A.H. Rezaeyan, A. Salajegheh, S. Rezapoor, Melatonin as an anti-inflammatory agent in radiotherapy, Inflammopharmacology 25 (2017) 403–413, https://doi.org/10.1007/s10787-017-0332-5.

[3] W.H.B. Wallace, A.B. Thomson, F. Saran, T.W. Kelsey, Predicting age of ovarian failure after radiation to a field that includes the ovaries, Int. J. Radiat. Oncol. Biol. Phys. 62 (2005) 738–744, https://doi.org/10.1016/j.ijrobp.2004.11.038.

[4] M. Vassilakopoulou, E. Boostandoost, G. Papaxoinis, T. de La Motte Rouge, D. Khayat, A. Psyrri, Anticancer treatment and fertility: effect of therapeutic modalities on reproductive system and functions, Crit. Rev. Oncol. Hematol. 97 (2016) 328–334, https://doi.org/10.1016/j.critrevonc.2015.08.002.

[5] M.K. Janiak, M. Wincenciak, A. Cheda, E.M. Nowosielska, E.J. Calabrese, Cancer immunotherapy: how low-level ionizing radiation can play a key role, Cancer Immunol. Immunother. 66 (2017) 819–832, https://doi.org/10.1007/s00262-017-1993-z.

[6] M. Martin, J. Lefaix, S. Delanian, TGF-beta1 and radiation fibrosis: a master switch and a specific therapeutic target? Int. J. Radiat. Oncol. Biol. Phys. 47 (2000) 277–290 (Accessed July 30, 2018), http://www.ncbi.nlm.nih.gov/pubmed/10802350.

[7] C. Boots, E. Jungheim, Inflammation and Human Ovarian Follicular Dynamics, Semin. Reprod. Med. 33 (2015) 270–275, https://doi.org/10.1055/s-0035-1554928.

[8] R.S. Said, E. El-Demerdash, A.S. Nada, M.M. Kamal, Resveratrol inhibits inflammatory signaling implicated in ionizing radiation-induced premature ovarian failure through antagonistic crosstalk between silencing information regulator 1 (SIRT1) and poly(ADP-ribose) polymerase 1 (PARP-1), Biochem. Pharmacol. 103 (2016) 140–150, https://doi.org/10.1016/j.bcp.2016.01.019.

[9] S.A. Haeri, H. Rajabi, S. Fazelipour, S.J. Hosseinimehr, Carnosine mitigates apoptosis and protects testicular seminiferous tubules from gamma-radiation-induced injury in mice, Andrologia 46 (2014) 1041–1046, https://doi.org/10.1111/and.12193.

[10] C. Tingen, A. Kim, T.K. Woodruff, The primordial pool of follicles and nest breakdown in mammalian ovaries, Mol. Hum. Reprod. 15 (2009) 795–803, https://doi.org/10.1093/molehr/gap073.

[11] D.C. Krakauer, A. Mira, Mitochondria and germ-cell death, Nature 400 (1999) 125–126, https://doi.org/10.1038/22026.

[12] A.N. Hirshfield, Size-frequency analysis of atresia in cycling rats, Biol. Reprod. 38 (1988) 1181–1188 (Accessed April 18, 2017), http://www.ncbi.nlm.nih.gov/pubmed/3408785.

[13] S.J. Hosseinimehr, The use of angiotensin II receptor antagonists to increase the efficacy of radiotherapy in cancer treatment, Future Oncol. 10 (2014) 2381–2390, https://doi.org/10.2217/fon.14.177.

[14] D. Meirow, D. Nugent, The effects of radiotherapy and chemotherapy on female reproduction, Hum. Reprod. Update 7 (2001) 535–543 (accessed April 17, 2017), http://www.ncbi.nlm.nih.gov/pubmed/11727861.

[15] M. Cheki, E. Mihandoost, A. Shirazi, A. Mahmoudzadeh, Prophylactic role of some plants and phytochemicals against radio-genotoxicity in human lymphocytes, J. Cancer Res. Ther. 12 (2016) 1234, https://doi.org/10.4103/0973-1482.172131.

[16] L. Song, L. Ma, F. Cong, X. Shen, P. Jing, X. Ying, H. Zhou, J. Jiang, Y. Fu, H. Yan, Radioprotective effects of genistein on HL-7702 cells via the inhibition of apoptosis and DNA damage, Cancer Lett. 366 (2015) 100–111, https://doi.org/10.1016/j.canlet.2015.06.008.

[17] U. Das, K. Manna, A. Khan, M. Sinha, S. Biswas, A. Sengupta, A. Chakraborty, S. Dey, Ferulic acid (FA) abrogates γ-radiation induced oxidative stress and DNA damage by up-regulating nuclear translocation of Nrf2 and activation of NHEJ pathway, Free Radic. Res. 51 (2017) 47–63, https://doi.org/10.1080/10715762.2016.1267345.

[18] N.F. Khedr, Protective effect of mirtazapine and hesperidin on cyclophosphamide-induced oxidative damage and infertility in rat ovaries, Exp. Biol. Med. 240 (2015) 1682–1689, https://doi.org/10.1177/1535370215576304.

[19] N.-L. Wu, J.-Y. Fang, M. Chen, C.-J. Wu, C.-C. Huang, C.-F. Hung, Chrysin Protects Epidermal Keratinocytes from UVA- and UVB-Induced Damage, J. Agric. Food Chem. 59 (2011) 8391–8400, https://doi.org/10.1021/jf200931t.

[20] E.M. Mantawy, W.M. El-Bakly, A. Esmat, A.M. Badr, E. El-Demerdash, Chrysin alleviates acute doxorubicin cardiotoxicity in rats via suppression of oxidative stress, inflammation and apoptosis, Eur. J. Pharmacol. 728 (2014) 107–118, https://doi.org/10.1016/j.ejphar.2014.01.065.

[21] N. Rani, S. Bharti, J. Bhatia, T.C. Nag, R. Ray, D.S. Arya, Chrysin, a PPAR-γ agonist improves myocardial injury in diabetic rats through inhibiting AGE-RAGE mediated oxidative stress and inflammation, Chem. Biol. Interact. 250 (2016) 59–67, https://doi.org/10.1016/j.cbi.2016.03.015.

[22] N. Rani, S. Bharti, J. Bhatia, A. Tomar, T.C. Nag, R. Ray, D. Arya, Inhibition of TGF-β by a novel PPAR-γ agonist, chrysin, salvages β-receptor stimulated myocardial injury in rats through MAPKs-dependent mechanism, Nutr. Metab. (Lond). 12 (2015) 11, https://doi.org/10.1186/s12986-015-0004-7.

[23] A. Salimi, M.H. Roudkenar, E. Seydi, L. Sadeghi, A. Mohseni, N. Pirahmadi, J. Pourahmad, Chrysin as an anti-cancer agent exerts selective toxicity by directly inhibiting mitochondrial complex II and V in CLL B-lymphocytes, Cancer Invest. 35 (2017) 174–186, https://doi.org/10.1080/07357907.2016.1276187.

[24] V. Benković, N. Orsolić, A.H. Knezević, S. Ramić, D. Dikić, I. Basić, N. Kopjar, Evaluation of the radioprotective effects of propolis and flavonoids in gamma-irradiated mice: the alkaline comet assay study, Biol. Pharm. Bull. 31 (2008) 167–172 (Accessed April 20, 2017), http://www.ncbi.nlm.nih.gov/pubmed/18175964.

[25] N. Orsolić, V. Benković, A. Horvat-Knezević, N. Kopjar, I. Kosalec, M. Bakmaz, Z. Mihaljević, K. Bendelja, I. Basić, Assessment by survival analysis of the radioprotective properties of propolis and its polyphenolic compounds, Biol. Pharm. Bull. 30 (2007) 946–951 (Accessed April 20, 2017), http://www.ncbi.nlm.nih.gov/pubmed/17473440.

[26] O. Ciftci, İ. Ozdemir, M. Aydin, A. Beytur, Beneficial effects of chrysin on the reproductive system of adult male rats, Andrologia 44 (2012) 181–186, https://doi.org/10.1111/j.1439-0272.2010.01127.x.

[27] E.H. Aksu, M. Özkaraca, F.M. Kandemir, A.D. Ömür, E. Eldutar, S. Küçükler, S. Çomaklı, Mitigation of paracetamol-induced reproductive damage by chrysin in male rats via reducing oxidative stress, Andrologia 48 (2016) 1145–1154, https://doi.org/10.1111/and.12553.

[28] K.L. Britt, A.E. Drummond, V.A. Cox, M. Dyson, N.G. Wreford, M.E. Jones, E.R. Simpson, J.K. Findlay, An age-related ovarian phenotype in mice with targeted disruption of the Cyp 19 (aromatase) gene, Endocrinology 141 (2000) 2614–2623, https://doi.org/10.1210/endo.141.7.7578.

[29] R.H. Braw, A. Tsafriri, Effect of PMSG on follicular atresia in the immature rat ovary, J. Reprod. Fertil. 59 (1980) 267–272 (Accessed May 20, 2017), http://www.ncbi.nlm.nih.gov/pubmed/7431285.

[30] H. Jang, K. Hong, Y. Choi, Melatonin and fertoprotective adjuvants: prevention against premature ovarian failure during chemotherapy, Int. J. Mol. Sci. 18 (2017) 1221, https://doi.org/10.3390/ijms18061221.

[31] K.M. Ataya, J.A. McKanna, A.M. Weintraub, M.R. Clark, W.J. LeMaire, A luteinizing hormone-releasing hormone agonist for the prevention of chemotherapy-induced ovarian follicular loss in rats, Cancer Res. 45 (1985) 3651–3656 (Accessed June 29, 2017), http://www.ncbi.nlm.nih.gov/pubmed/3926307.

[32] K. Miyazaki, F. Miki, S. Uchida, H. Masuda, H. Uchida, T. Maruyama, Serum estradiol level during withdrawal bleeding as a predictive factor for intermittent ovarian function in women with primary ovarian insufficiency, Endocr. J. 62 (2015) 93–99, https://doi.org/10.1507/endocrj.EJ14-0189.

[33] R.S. Said, A.S. Nada, E. El-Demerdash, sodium selenite improves folliculogenesis in radiation-induced ovarian failure: a mechanistic approach, PLoS One 7 (2012) e50928, https://doi.org/10.1371/journal.pone.0050928.

[34] J.B. Kerr, L. Brogan, M. Myers, K.J. Hutt, T. Mladenovska, S. Ricardo, K. Hamza, C.L. Scott, A. Strasser, J.K. Findlay, The primordial follicle reserve is not renewed after chemical or -irradiation mediated depletion, Reproduction 143 (2012) 469–476, https://doi.org/10.1530/REP-11-0430.

[35] R.C. Langan, P.A. Prieto, R.M. Sherry, D. Zlott, J. Wunderlich, G. Csako, R. Costello, D.E. White, S.A. Rosenberg, J.C. Yang, Assessment of ovarian function after preparative chemotherapy and total body radiation for adoptive cell therapy, J. Immunother. 34 (2011) 397–402, https://doi.org/10.1097/CJI.0b013e3182187508.

[36] C. Aktas, M. Kanter, Z. Kocak, Antiapoptotic and proliferative activity of curcumin on ovarian follicles in mice exposed to whole body ionizing radiation, Toxicol. Ind. Health 28 (2012) 852–863, https://doi.org/10.1177/0748233711425080.

[37] H.-M. Zhou, Q.-X. Sun, Y. Cheng, Paeonol enhances the sensitivity of human ovarian cancer cells to radiotherapy-induced apoptosis due to downregulation of the phosphatidylinositol-3-kinase/Akt/phosphatase and tensin homolog pathway and inhibition of vascular endothelial growth factor, Exp. Ther. Med. 14 (2017) 3213–3220, https://doi.org/10.3892/etm.2017.4877.

[38] J. Yang, S. Hu, M. Rao, L. Hu, H. Lei, Y. Wu, Y. Wang, D. Ke, W. Xia, C.-H. Zhu, Copper nanoparticle-induced ovarian injury, follicular atresia, apoptosis, and gene expression alterations in female rats, Int. J. Nanomedicine 12 (2017) 5959–5971, https://doi.org/10.2147/IJN.S139215.

[39] F. Kandemir, S. Kucukler, E. Eldutar, C. Caglayan, İ. Gülçin, chrysin protects rat kidney from paracetamol-induced oxidative stress, inflammation, apoptosis, and autophagy: a multi-biomarker approach, Sci. Pharm. 85 (2017) 4, https://doi.org/10.3390/scipharm85010004.

[40] E.M. Mantawy, A. Esmat, W.M. El-Bakly, R.A. Salah ElDin, E. El-Demerdash, Mechanistic clues to the protective effect of chrysin against doxorubicin-induced cardiomyopathy: Plausible roles of p53, MAPK and AKT pathways, Sci. Rep. 7 (2017) 4795, https://doi.org/10.1038/s41598-017-05005-9.

[41] Y. Wang, X. Tian, L. Liang, Y. Wang, R. Wang, X. Cheng, Z. Yan, Y. Chen, P. Qi, Mechanistic Study on Triptorelin Action in Protecting From 5-FU-Induced Ovarian Damage in Rats, Oncol. Res. 22 (2014) 283–292, https://doi.org/10.3727/096504015X14410238486720.

[42] Y. Bayir, E. Cadirci, B. Polat, N. Kilic Baygutalp, A. Albayrak, E. Karakus, H. Un, M.S. Keles, F.B. Kocak Ozgeris, E. Toktay, M. Karaca, Z. Halici, Aliskiren - a promising strategy for ovarian ischemia/reperfusion injury protection in rats via RAAS, Gynecol. Endocrinol. 32 (2016) 675–683, https://doi.org/10.3109/09513590.2016.1153055.

[43] E. kaygusuzoglu, C. Caglayan, F.M. Kandemir, S. Yıldırım, S. Kucukler, M.A. Kılınc, Y.S. Saglam, Zingerone ameliorates cisplatin-induced ovarian and uterine toxicity via suppression of sex hormone imbalances, oxidative stress, inflammation and apoptosis in female wistar rats, Biomed. Pharmacother. 102 (2018) 517–530, https://doi.org/10.1016/j.biopha.2018.03.119.

[44] C. Linard, A. Ropenga, M.C. Vozenin-Brotons, A. Chapel, D. Mathe, Abdominal irradiation increases inflammatory cytokine expression and activates NF-kappaB in rat ileal muscularis layer, Am. J. Physiol. Gastrointest. Liver Physiol. 285 (2003) G556–565, https://doi.org/10.1152/ajpgi.00094.2003.

[45] Y. Zhang, L. Gao, Z. Cheng, J. Cai, Y. Niu, W. Meng, Q. Zhao, Kukoamine A Prevents Radiation-Induced Neuroinflammation and Preserves Hippocampal Neurogenesis in

Rats by Inhibiting Activation of NF-κB and AP-1, Neurotox. Res. 31 (2017) 259–268, https://doi.org/10.1007/s12640-016-9679-4.
[46] J.S. Russell, P.J. Tofilon, Radiation-induced activation of nuclear factor-kappaB involves selective degradation of plasma membrane-associated I(kappa)B(alpha), Mol. Biol. Cell 13 (2002) 3431–3440, https://doi.org/10.1091/mbc.e02-05-0252.
[47] M.R. Akanda, H.-H. Nam, W. Tian, A. Islam, B.-K. Choo, B.-Y. Park, Regulation of JAK2/STAT3 and NF-κB signal transduction pathways; Veronica polita alleviates dextran sulfate sodium-induced murine colitis, Biomed. Pharmacother. 100 (2018) 296–303, https://doi.org/10.1016/j.biopha.2018.01.168.
[48] K.V. Premkumar, S.K. Chaube, Nitric oxide signals postovulatory aging-induced abortive spontaneous egg activation in rats, Redox Rep. 20 (2015) 184–192, https://doi.org/10.1179/1351000215Y.0000000003.
[49] Q. Luo, N. Yin, L. Zhang, W. Yuan, W. Zhao, X. Luan, H. Zhang, Role of SDF-1/CXCR4 and cytokines in the development of ovary injury in chemotherapy drug induced premature ovarian failure mice, Life Sci. 179 (2017) 103–109, https://doi.org/10.1016/j.lfs.2017.05.001.
[50] M. Zeinali, S.A. Rezaee, H. Hosseinzadeh, An overview on immunoregulatory and anti-inflammatory properties of chrysin and flavonoids substances, Biomed. Pharmacother. 92 (2017) 998–1009, https://doi.org/10.1016/j.biopha.2017.06.003.
[51] G.C. Blobe, W.P. Schiemann, H.F. Lodish, Role of transforming growth factor beta in human disease, N. Engl. J. Med. 342 (2000) 1350–1358, https://doi.org/10.1056/NEJM200005043421807.
[52] S.A. Pangas, Regulation of the ovarian reserve by members of the transforming growth factor beta family, Mol. Reprod. Dev. 79 (2012) 666–679, https://doi.org/10.1002/mrd.22076.
[53] L. Fang, H.-M. Chang, J.-C. Cheng, P.C.K. Leung, Y.-P. Sun, TGF-β1 downregulates StAR expression and decreases progesterone production through Smad3 and ERK1/2 signaling pathways in human granulosa cells, J. Clin. Endocrinol. Metab. 99 (2014) E2234–43, https://doi.org/10.1210/jc.2014-1930.
[54] D. Rosairo, I. Kuyznierewicz, J. Findlay, A. Drummond, Transforming growth factor- : its role in ovarian follicle development, Reproduction 136 (2008) 799–809, https://doi.org/10.1530/REP-08-0310.
[55] C.E. Rube, D. Uthe, K.W. Schmid, K.D. Richter, J. Wessel, A. Schuck, N. Willich, C. Rube, Dose-dependent induction of transforming growth factor beta (TGF-beta) in the lung tissue of fibrosis-prone mice after thoracic irradiation, Int. J. Radiat. Oncol. Biol. Phys. 47 (2000) 1033–1042 (Accessed July 31, 2018), http://www.ncbi.nlm.nih.gov/pubmed/10863076.
[56] K. Miyazono, P. ten Dijke, C.H. Heldin, TGF-beta signaling by Smad proteins, Adv. Immunol. 75 (2000) 115–157 (Accessed February 18, 2018), http://www.ncbi.nlm.nih.gov/pubmed/10879283.
[57] X. Guo, X.-F. Wang, Signaling cross-talk between TGF-beta/BMP and other pathways, Cell Res. 19 (2009) 71–88, https://doi.org/10.1038/cr.2008.302.
[58] L. Chang, M. Karin, Mammalian MAP kinase signalling cascades, Nature 410 (2001) 37–40, https://doi.org/10.1038/35065000.
[59] G.L. Johnson, R. Lapadat, Mitogen-activated protein kinase pathways mediated by ERK, JNK, and p38 protein kinases, Science 298 (2002) 1911–1912, https://doi.org/10.1126/science.1072682.
[60] A. Plotnikov, E. Zehorai, S. Procaccia, R. Seger, The MAPK cascades: signaling components, nuclear roles and mechanisms of nuclear translocation, Biochim. Biophys. Acta 1813 (2011) 1619–1633, https://doi.org/10.1016/j.bbamcr.2010.12.012.
[61] F.C. Barone, E.A. Irving, A.M. Ray, J.C. Lee, S. Kassis, S. Kumar, A.M. Badger, J.J. Legos, J.A. Erhardt, E.H. Ohlstein, A.J. Hunter, D.C. Harrison, K. Philpott, B.R. Smith, J.L. Adams, A.A. Parsons, Inhibition of p38 mitogen-activated protein kinase provides neuroprotection in cerebral focal ischemia, Med. Res. Rev. 21 (2001) 129–145 (accessed July 31, 2018), http://www.ncbi.nlm.nih.gov/pubmed/11223862.
[62] K. Schulze-Osthoff, D. Ferrari, K. Riehemann, S. Wesselborg, Regulation of NF-kappa B activation by MAP kinase cascades, Immunobiology 198 (1997) 35–49 (Accessed July 31, 2018), http://www.ncbi.nlm.nih.gov/pubmed/9442376.
[63] A. Wullaert, K. Heyninck, R. Beyaert, Mechanisms of crosstalk between TNF-induced NF-kappaB and JNK activation in hepatocytes, Biochem. Pharmacol. 72 (2006) 1090–1101, https://doi.org/10.1016/j.bcp.2006.07.003.
[64] T. Wada, J.M. Penninger, Mitogen-activated protein kinases in apoptosis regulation, Oncogene. 23 (2004) 2838–2849, https://doi.org/10.1038/sj.onc.1207556.
[65] J. Uma, P. Muraly, S. Verma-Kumar, R. Medhamurthy, Determination of onset of apoptosis in granulosa cells of the preovulatory follicles in the bonnet monkey (Macaca radiata): correlation with mitogen-activated protein kinase activities, Biol. Reprod. 69 (2003) 1379–1387, https://doi.org/10.1095/biolreprod.103.017897.
[66] X. Hu, J.A. Flaws, I.G. Sipes, P.B. Hoyer, Activation of mitogen-activated protein kinases and AP-1 transcription factor in ovotoxicity induced by 4-vinylcyclohexene diepoxide in rats, Biol. Reprod. 67 (2002) 718–724 (Accessed July 31, 2018), http://www.ncbi.nlm.nih.gov/pubmed/12193377.
[67] V. Subramanian, S. Borchard, O. Azimzadeh, W. Sievert, J. Merl-Pham, M. Mancuso, E. Pasquali, G. Multhoff, B. Popper, H. Zischka, M.J. Atkinson, S. Tapio, PPARα Is Necessary for Radiation-Induced Activation of Noncanonical TGFβ Signaling in the Heart, J. Proteome Res. 17 (2018) 1677–1689, https://doi.org/10.1021/acs.jproteome.8b00001.
[68] J. Ahamed, J. Laurence, Role of platelet-derived transforming growth Factor-β1 and reactive oxygen species in radiation-induced organ fibrosis, Antioxid. Redox Signal. 27 (2017) 977–988, https://doi.org/10.1089/ars.2017.7064.
[69] R. Asur, M. Balasubramaniam, B. Marples, R.A. Thomas, J.D. Tucker, Involvement of MAPK proteins in bystander effects induced by chemicals and ionizing radiation, Mutat. Res. Mol. Mech. Mutagen. 686 (2010) 15–29, https://doi.org/10.1016/j.mrfmmm.2009.12.007.